Broadband wavelength converters with flattop responses based on cascaded second-harmonic generation and difference frequency generation in Bessel-chirped gratings

Tao Liu,[1,2,*] Ivan B. Djordjevic,[2] Zekun Song,[1] Ying Chen,[1] Rongxiang Zhang,[3] Ke Zhang,[1] Wei Zhao,[1] and Baogang Li[1]

[1]*Department of Electronic and Communication Engineering, North China Electric Power University, Yong Hua North Street, Hebei Baoding 071003, China*

[2]*Department of Electrical and Computer Engineering, University of Arizona, 1230 E Speedway Blvd., Tucson, Arizona 85721, USA*

[3]*College of Physics Science and Technology, Hebei University, Wu Si East Road, Hebei Baoding 071002, China*

[*]*taoliu@ncepu.edu.cn*

Abstract: We investigate ultra-broadband wavelength converters based on cascaded second-harmonic generation and difference frequency generation using Bessel-chirped gratings (BCGs) in lithium niobate waveguides, and compare them to the ones using uniform grating and segmented grating, respectively. For the same length and power, the BCGs show broader bandwidth than the other two types of grating. The ripple of the matching response is very small as well. Analysis also shows that almost the same conversion bandwidth and maximum conversion efficiency with tolerant response flatness can be achieved when the manufacturing tolerance of the waveguide length is smaller than 0.1 cm.

OCIS codes: (190.0190) Nonlinear optics; (190.2620) Harmonic generation and mixing; (190.4360) Nonlinear optics, devices; (190.4410) Nonlinear optics, parametric processes.

References and links

1. S. J. B. Yoo, "Wavelength conversion technologies for WDM network applications," J. Lightwave Technol. **14**(6), 955–966 (1996).
2. C. Q. Xu, H. Okayama, and M. Kawahara, "1.5 μm band efficient broadband wavelength conversion by difference frequency generation in a periodically domain-inverted $LiNbO_3$ channel waveguide," Appl. Phys. Lett. **63**(26), 3559–3561 (1993).
3. M. H. Chou, J. Hauden, M. A. Arbore, and M. M. Fejer, "1.5- μm -band wavelength conversion based on difference-frequency generation in $LiNbO_3$ waveguides with integrated coupling structures," Opt. Lett. **23**(13), 1004–1006 (1998).
4. A. J. Torregrosa, H. Maestre, and J. Capmany, "Wavelength conversion of incoherent broadband sources by intracavity difference frequency mixing," IEEE Photonics Technol. Lett. **26**(7), 694–697 (2014).
5. G. W. Lu, A. Albuquerque, B. J. Puttnam, T. Sakamoto, M. Drummond, R. Nogueira, A. Kanno, S. Shinada, N. Wada, and T. Kawanishi, "Pump-linewidth-tolerant optical wavelength conversion for high-order QAM signals using coherent pumps," Opt. Express **22**(5), 5067–5075 (2014).
6. C. Langrock, S. Kumar, J. E. McGeehan, A. E. Willner, and M. M. Fejer, "All-optical signal processing using $\chi^{(2)}$ nonlinearities in guided-wave devices," J. Lightwave Technol. **24**(7), 2579–2592 (2006).
7. G. W. Lu, S. Shinada, H. Furukawa, N. Wada, T. Miyazaki, and H. Ito, "160-Gb/s all-optical phase-transparent wavelength conversion through cascaded SFG-DFG in a broadband linear-chirped PPLN waveguide," Opt. Express **18**(6), 6064–6070 (2010).
8. M. H. Chou, I. Brener, M. M. Fejer, E. E. Chaban, and S. B. Christman, "1.5-μm-band wavelength conversion based on cascaded second-order nonlinearity in $LiNbO_3$ waveguides," IEEE Photonics Technol. Lett. **11**(6), 653–655 (1999).
9. S. Yu and W. Gu, "Wavelength conversions in quasi-phase matched $LiNbO_3$ waveguide based on double-pass cascaded $\chi^{(2)}$ SFG + DFG interactions," IEEE J. Quantum Electron. **40**(11), 1548–1554 (2004).

#262298 Received 4 Apr 2016; revised 4 May 2016; accepted 6 May 2016; published 10 May 2016

10. T. Liu, Y. Qi, L. Che, B. Li, S. Yu, and W. Gu, "Flat broadband wavelength conversion based on cascaded second-harmonic generation and difference frequency generation in segmented quasi-phase matched gratings," J. Mod. Opt. **59**(7-8), 650–657 (2012).
11. X. Liu, H. Zhang, Y. Guo, and Y. Li, "Optimal design and applications for quasi-phase-matching three-wave mixing," IEEE J. Quantum Electron. **38**(9), 1225–1233 (2002).
12. W. Liu, J. Sun, and J. Kurz, "Bandwidth and tenability enhancement of wavelength conversion by quasi-phase-matching difference frequency generation," Opt. Commun. **216**(1–3), 239–246 (2003).
13. A. Tehranchi, R. Morandotti, and R. Kashyap, "Efficient flattop ultra-wideband wavelength converters based on double-pass cascaded sum and difference frequency generation using engineered chirped gratings," Opt. Express **19**(23), 22528 (2011).
14. S. Gao, C. Yang, and G. Jin, "Flat broad-band wavelength conversion based on sinusoidally chirped optical superlattices in lithium niobate," IEEE Photonics Technol. Lett. **16**(2), 557–559 (2004).
15. J. Wang, J. Sun, X. Zhang, D. Huang, and M. M. Fejer, "All-optical format conversions using periodically poled lithium niobate waveguides," IEEE J. Quantum Electron. **45**(2), 195–205 (2009).
16. F. D. Ros, K. Dalgaard, Y. Fukuchi, J. Xu, M. Galili, and C. Peucheret, "Simultaneous QPSK-to-2×BPSK wavelength and modulation format conversion in PPLN," IEEE Photon. Technol. Lett. **26**(12), 1207–1210 (2014).
17. M. Ahlawat, A. Tehranchi, K. Pandiyan, M. Cha, and R. Kashyap, "Tunable all-optical wavelength broadcasting in a PPLN with multiple QPM peaks," Opt. Express **20**(24), 27425–27433 (2012).
18. G. Meloni, V. Vercesi, M. Scaffardi, A. Bogoni, and L. Poti, "Spectral-efficient flexible optical multicasting in a periodically poled lithium niobate waveguide," J. Lightwave Technol. **33**(23), 4731–4737 (2015).
19. E. Lazzeri, A. Malacarne, G. Serafino, and A. Bogoni, "Optical XOR for error detection and coding of QPSK I and Q components in PPLN waveguide," IEEE Photonics Technol. Lett. **24**(24), 2258–2261 (2012).
20. H. Kanbara, H. Itoh, M. Asobe, K. Noguchi, H. Miyazawa, T. Yanagawa, and I. Yokohama, "All-optical switching based on cascading of secondorder nonlinearities in a periodically poled titanium-diffused lithium niobate waveguide," IEEE Photon. Technol. Lett. **11**(3), 328–330 (1999).
21. G. S. Kanter, P. Kumar, K. R. Parameswaran, and M. M. Fejer, "Wavelength-selective pulsed all-optical switching based on cascaded secondorder nonlinearity in a periodically poled lithium-niobate waveguide," IEEE Photonics Technol. Lett. **13**(4), 341–343 (2001).
22. S. Kurimura, Y. Kato, M. Maruyama, Y. Usui, and H. Nakajima, "Quasi-phase-matched adhered ridge waveguide in $LiNbO_3$," Appl. Phys. Lett. **89**(19), 191123 (2006).
23. R. Kou, S. Kurimura, K. Kikuchi, A. Terasaki, H. Nakajima, K. Kondou, and J. Ichikawa, "High-gain, wide-dynamic-range parametric interaction in Mg-doped $LiNbO_3$ quasi-phase-matched adhered ridge waveguide," Opt. Express **19**(12), 11867–11872 (2011).
24. D. H. Jundt, "Temperature-dependent Sellmeier equation for the index of refraction, $n_{(e)}$, in congruent lithium niobate," Opt. Lett. **22**(20), 1553–1555 (1997).
25. K. Gallo and G. Assanto, "Analysis of lithium niobate all-optical wavelength shifters for the third spectral window," J. Opt. Soc. Am. B **16**(5), 741–753 (1999).
26. S. Gao, C. Yang, X. Xiao, Y. Tian, Z. You, and G. Jin, "Performance evaluation of tunable channel-selective wavelength shift by cascaded sum- and difference-frequency generation in periodically poled lithium niobate waveguides," J. Lightwave Technol. **25**(3), 710–718 (2007).

1. Introduction

Recently, broadband wavelength converters based on second-order nonlinear-optical effect in quasi-phase matched (QPM) waveguides have attracted much attentions thank to their ultra-fast optical responses, large nonlinear coefficients, negligible spontaneous emission noise, low cross-talk and complete transparency [1–14]. Besides the wavelength conversion function, these devices can be also used to realize modulation format conversion [15,16], signal optical multicasting [17,18] and logical XOR operation [19]. Difference frequency generation [2–4] (DFG) is the simplest approach to achieve wavelength conversion in QPM waveguides. However, this scheme suffers from the following problem. When launching the 780 nm pump wave and the 1.5 μm signal wave into the waveguide simultaneously, the waveguide can typically only support quasi-TM_{00} mode in the 1.5-μm band. To overcome this problem, two schemes using cascaded second-harmonic generation and difference frequency generation (SHG + DFG) and cascaded sum and difference frequency generation (SFG + DFG) were proposed, respectively; and studied both theoretically and experimentally [6–9].

Typically, periodically poled lithium niobate (PPLN) fabricated by the technology of Ti diffusion [20] or annealed proton exchange [21] (APE) has been employed in wavelength converters. However, the conversion bandwidth of about 80 nm for such waveguides with uniform grating structure is very limited [2,3,11]. This will affects the multichannel

#262298 Received 4 Apr 2016; revised 4 May 2016; accepted 6 May 2016; published 10 May 2016

conversion in the wavelength division multiplexing (WDM) systems, which usually requires the conversion bandwidth to be as broad as possible to cover the whole communication band and the response should be flat enough so that no optical equalizer will be required to compensate the spectrum distortion after wavelength conversion takes place. Beside conversion bandwidth and response flatness, conversion efficiency is also an important characteristic for wavelength converters, and both of the conversion bandwidth and efficiency will vary with waveguide length. Generally, longer waveguides result to higher conversion efficiency but smaller conversion bandwidth [10, 14]. That is, broader conversion bandwidth can be obtained by using shorter waveguides with some conversion efficiency penalty. S. Kurimura and R. Kou [22,23] reported very high normalized conversion efficiency, $370\%W^{-1}cm^{-2}$ for SHG, by utilizing adhered-ridge-waveguide (ARW) devices. This efficiency is more than twice that of the typical APE devices in the telecommunication wavelength region, which means it is possible to obtain large conversion bandwidth by using short ARW instead of long APE waveguide for the same efficiency. Another effective method to broaden the conversion bandwidth is employing engineered QPM structures. By using segmented gratings, T. Liu [10] obtained enhanced conversion bandwidth. For 3-cm-long 3-segment PPLN, the bandwidth reaches 160 nm, −10.46 dB ($10\%W^{-1}cm^{-2}$) conversion efficiency is achieved simultaneously. X. Liu [11] demonstrated that, by taking advantage of segmented gratings and adding phase-shift sections between two adjacent segments, 10 nm additional conversion bandwidth can be obtained in comparison with that of using segmented gratings only, meanwhile the conversion efficiency of about −5 dB ($79\%W^{-1}cm^{-2}$) remains almost the same. However, the response in his schemes is saddle-like with large ripple. To flatten the response, A. Tehranchi [13] reported a step-chirped structure and obtained less than 0.2 dB response flatness and −16.1 dB ($5\%W^{-1}cm^{-2}$) conversion efficiency based on it, but the conversion bandwidth of about 95 nm is limited. S. Gao [14] proposed a sinusoidally chirped optical superlattice (SCOS) structure to widen the bandwidth as well as reduce the ripple on response. By using this structure in a 3-cm-long waveguide, he achieved 142 nm conversion bandwidth, −9.3 dB ($4\%W^{-1}cm^{-2}$) conversion efficiency, and 0.46 dB response flatness, respectively; but the bandwidth is still not sufficiently large.

In this paper, we present a novel Bessel-chirped gratings (BCGs) for wavelength converters based on cascaded SHG + DFG. By employing the BCGs, the conversion bandwidth can be greatly broadened, and flat response can be simultaneously obtained. Comparison among BCGs, uniform grating, and segmented grating is also carried out. The results show that conversion devices employing BCGs have broader bandwidth and smaller ripples. Furthermore, we evaluate the properties of BCGs-based devices with different waveguide lengths but same variation of poling period and show that almost the same combined performances can be obtained when the manufacturing tolerance of waveguide length is within 0.1 cm. Therefore, the proposed BCGs are suitable for fabrication.

2. Description of the proposed BCGs

The BCGs structure, as shown in Fig. 1, is implemented in a Z-cut and X-propagating lithium niobate channel waveguide. In the structure, the period changes according to the following function

$$\Lambda(x) = \Lambda_0 \left\{ 1 + \gamma J_v \left[\tau \left(\xi + \frac{x}{L} \right) \right] \right\}, \tag{1}$$

where J_v is Bessel functions of the first kind, v is the order of Bessel functions; γ, τ, and ξ are the chirp coefficients; L is the total waveguide length. The $\Lambda_0 = \lambda_p/(2N_{SH}-2N_p)$ is a period of the uniform QPM grating, where N_{SH} and N_p are model indices of the second harmonic (SH) wave and pump wave, respectively.

#262298 Received 4 Apr 2016; revised 4 May 2016; accepted 6 May 2016; published 10 May 2016

In this paper, we take the advantage of zero order Bessel function. That is, the order v in Eq. (1) is assumed to be 0. In this case, the poling periods of BCGs will change as the J_0 curve along x direction, as shown in Fig. 1. Through adjusting the chirp coefficients γ and τ, one can control the vertical scale and the oscillating period of J_0, respectively. In addition, by regulating the parameter ξ, the starting point on the horizontal axis of J_0 can be changed accordingly. Thus the variation of the QPM period is determined by these three coefficients. As a result, flattop broadband wavelength conversion can be realized by employing the proposed BCGs structure and optimizing γ, τ and ξ accordingly.

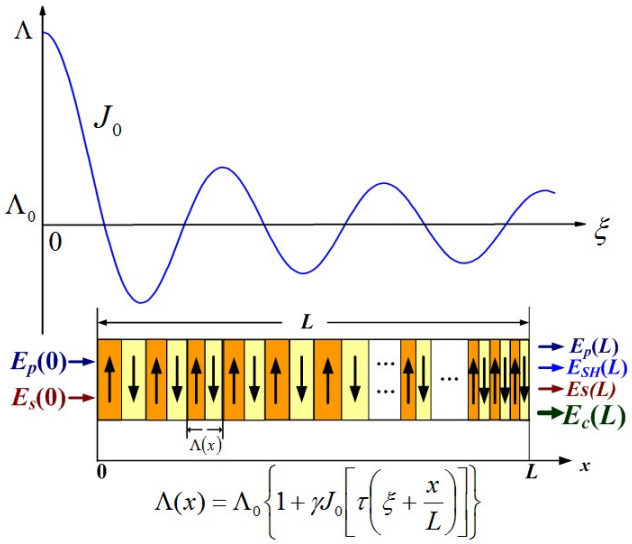

Fig. 1. Model of BCGs for cascaded SHG + DFG wavelength conversion.

In order to increase the conversion bandwidth and enhance the flatness of response, the BCGs is utilized in cascaded SHG + DFG wavelength conversion, as illustrated in Fig. 1. Employing the slowly varying envelope approximation [10], the cascaded SHG + DFG processes can be expressed by the following nonlinear coupled-mode equations:

$$\frac{\partial E_p}{\partial x} = -i\omega_p \kappa_{SHG} E_p^* E_{SH} \exp\left[-i\Delta\Phi_{SHG}(x)\right] - \frac{\alpha_p}{2} E_p, \tag{2}$$

$$\frac{\partial E_s}{\partial x} = -i\omega_s \kappa_{DFG} E_c^* E_{SH} \exp\left[-i\Delta\Phi_{DFG}(x)\right] - \frac{\alpha_s}{2} E_s, \tag{3}$$

$$\frac{\partial E_c}{\partial x} = -i\omega_c \kappa_{DFG} E_s^* E_{SH} \exp\left[-i\Delta\Phi_{DFG}(x)\right] - \frac{\alpha_c}{2} E_c, \tag{4}$$

$$\frac{\partial E_{SH}}{\partial x} = -i\omega_p \kappa_{SHG} E_p^2 \exp\left[i\Delta\Phi_{SHG}(x)\right] - i\omega_{SH} \kappa_{DFG} E_s E_c \exp\left[i\Delta\Phi_{DFG}(x)\right] - \frac{\alpha_{SH}}{2} E_{SH}, \tag{5}$$

where E_p, E_s, E_{SH}, E_c are the field amplitudes of pump wave, signal wave, SH wave and converted wave, respectively. The α_i (i = p, s, c or SH) is the propagation loss of ω_i. The $\kappa_{SHG} = d_{eff}\sqrt{2\mu_0} / \sqrt{CS_{SHG}N_p^2 N_{SH}}$ and $\kappa_{DFG} = d_{eff}\sqrt{2\mu_0} / \sqrt{CS_{DFG}N_S N_C N_{SH}}$ are the nonlinear coupling constants, where N_i denotes the modal index at ω_i and can be calculated by using Sellmeier equation [24], C is the light speed in vacuum and d_{eff} = $(2/\pi)$ d_{33} is the effective value of the nonlinear coefficient, and d_{33} parameter of lithium niobate is ≈27 pm/V [25].

#262298 Received 4 Apr 2016; revised 4 May 2016; accepted 6 May 2016; published 10 May 2016

Additionally, S_{SHG} and S_{DFG} are the effective interaction areas for SHG and DFG and are calculated to be $S_{SHG} \approx S_{DFG} \approx 47\ \mu m^2$ using mode overlap integral of the mode field distributions [25]. The phase mismatches are $\Delta\Phi_{SHG}(x) = \left(\beta_{SH} - 2\beta_p\right)x - \int_0^x 2\pi / \Lambda(x)dx$ and $\Delta\Phi_{DFG}(x) = (\beta_{SH} - \beta_s - \beta_c)x - \int_0^x 2\pi / \Lambda(x)dx$. The conversion efficiency is defined as $\eta = 10 \times \log[P_c(L)/P_s(0)]$, where P_s and P_c are the powers of input and converted signals respectively.

3. BCGs design results and discussion

Based on the above theoretical models, the performances of wavelength converters using cascaded SHG + DFG interaction in BCGs waveguide are discussed in this section. Moreover, comparison among BCGs, uniform grating, and segmented grating [10] is carried out in terms of conversion bandwidth, conversion efficiency and the flatness of response. Neglecting the waveguide loss, Fig. 2 depicts the conversion efficiencies of proposed BCGs against using uniform grating, and 3-segment grating. Here the signal power is 1 mW, the pump is 150 mW at 1.55 μm, the total waveguide length is 3 cm, and the temperature is taken to be 150°C. The QPM period Λ_0, used in Eq. (1), is calculated to be 18.511 μm when the SHG interaction is perfectly phase matched. The coupling constants used in Eqs. (2)-(5) are calculated as $\kappa_{SHG} \approx \kappa_{DFG} \approx 0.87\ W^{-1/2}cm^{-1}$, i.e., the value of κ^2_{SHG} and κ^2_{DFG} corresponding to the normalized conversion efficiency is approximately equal to $76\%W^{-1}cm^{-2}$. An interesting figure of merit to compare different wavelength converters, the response flatness, is defined as $F = \eta_{max} - \eta_{mean}$, where η_{max} and η_{mean} are maximum and mean conversion efficiencies within 3-dB bandwidth, respectively. Smaller flatness indicates that corresponding response is more flat.

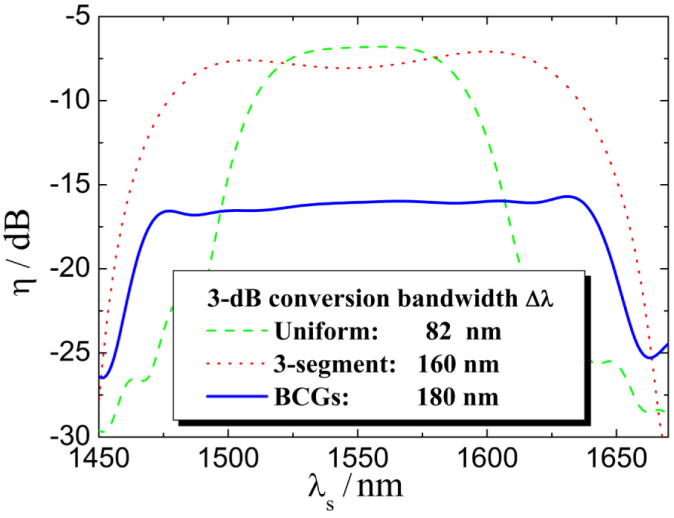

Fig. 2. Conversion efficiencies versus the signal wavelength in uniform grating, 3-segment grating and BCGs when the total waveguide length L equals 3 cm.

#262298 Received 4 Apr 2016; revised 4 May 2016; accepted 6 May 2016; published 10 May 2016

Table 1. Chirp coefficients γ, τ, and ξ and the corresponding conversion properties for various waveguide lengths *L*

L/ cm	scheme (a)						scheme (b)					
	γ	τ	ξ	$\Delta\lambda$/ nm	η_{max}/ dB	*F*/ dB	γ	τ	ξ	$\Delta\lambda$/ nm	η_{max}/ dB	*F*/ dB
1	0.008320			311	-33.50	0.71	0.004417			310	-33.52	0.89
1.5	0.005632			254	-26.77	0.65	0.003009			254	-26.87	0.77
2	0.004224			220	-21.95	0.64	0.002269			219	-22.13	0.71
2.5	0.003456			198	-18.53	0.55	0.001837			196	-18.59	0.65
3	0.002944	11.2	7.2	180	-15.67	0.62	0.001536	11.2	1.6	179	-15.70	0.62
3.5	0.002560			167	-13.34	0.62	0.001332			166	-13.38	0.57
4	0.002176			156	-11.10	0.54	0.001174			155	-11.37	0.57
4.5	0.001920			147	-9.29	0.67	0.001038			145	-9.45	0.62
5	0.001792			140	-8.05	0.47	0.000956			139	-8.21	0.50
L/ cm	scheme (c)						scheme (d)					
	γ	τ	ξ	$\Delta\lambda$/ nm	η_{max}/ dB	*F*/ dB	γ	τ	ξ	$\Delta\lambda$/ nm	η_{max}/ dB	*F*/ dB
1	0.008704			264	-32.00	0.58	0.008832			260	-32.10	0.57
1.5	0.005888			215	-25.14	0.55	0.006016			213	-25.25	0.58
2	0.004480			186	-20.28	0.61	0.004480			183	-20.35	0.57
2.5	0.003584			166	-16.58	0.58	0.003456			160	-16.32	0.63
3	0.002944	8	10.4	151	-13.52	0.54	0.003013	8	11.2	149	-13.62	0.58
3.5	0.002560			140	-11.06	0.56	0.002560			137	-11.13	0.48
4	0.002176			128	-8.69	0.56	0.002200			128	-8.86	0.50
4.5	0.001920			119	-6.70	0.58	0.001984			121	-7.07	0.45
5	0.001792			115	-5.29	0.53	0.001786			114	-5.37	0.42

To obtain flat broadband wavelength conversion, the chirp coefficients γ, τ and ξ are optimized in terms of conversion bandwidth and response flatness in the processes of calculating conversion efficiencies using Eqs. (2)-(5). The response flatness *F* is assumed to be less than 0.75 dB, in the simulation throughout this paper, to ensure flat matching response can be achieved. Under this restriction, several combinations of chirp coefficients and the corresponding wavelength conversion properties are obtained and shown in Table 1. It can be seen from Table 1 that, the conversion bandwidths corresponding to schemes (c) and (d) are both much less than those of schemes (a) and (b), for the same waveguide length. Further comparing scheme (a) with (b) we can find that, although almost the same bandwidth and maximum conversion efficiency can be achieved by using scheme (b) in comparison to those of scheme (a), under the same condition, the response flatness of the former is worse than that of the latter for short waveguide cases ($L \leq 2$cm). Therefore, the chirp coefficients determined for scheme (a) can be considered as the optimal chirp coefficients and utilized here to obtain broadened conversion bandwidth with flattened response.

It is evident from Fig. 2 that the 3-dB conversion bandwidth $\Delta\lambda$ in the BCGs structure is broader than that of the uniform grating and 3-segment grating. The ripple on the response is very small as well. For 3-cm-long waveguide, the bandwidths $\Delta\lambda$ are 180 nm, 160 nm and 82 nm, and the flatness *F* are 0.62 dB, 0.82 dB and 0.64 dB, for BCGs, 3-segment and uniform gratings, respectively. The 180 nm bandwidth covers almost the whole S-band, the whole C-band and L-band, and a half of U-band.

#262298 Received 4 Apr 2016; revised 4 May 2016; accepted 6 May 2016; published 10 May 2016

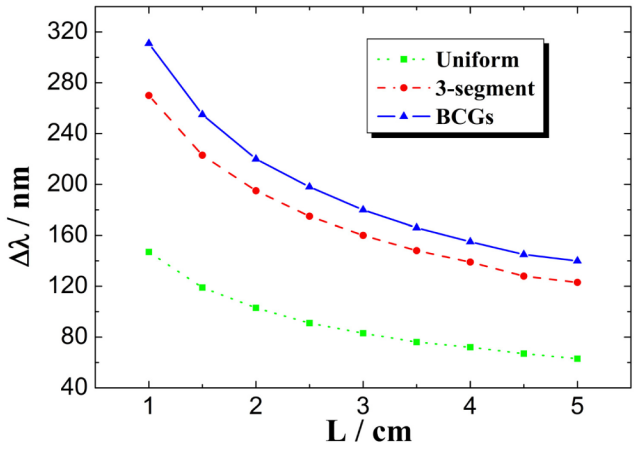

Fig. 3. Conversion bandwidths versus the total waveguide length in uniform grating, 3-segment grating and BCGs.

It is important that the proposed BCGs structure should be suitable for different waveguide lengths to ensure that the same wavelength conversion properties can be obtained no matter what the length is. Therefore, the performances of BCGs-based wavelength converters are investigated by varying the total waveguide length. The corresponding comparison among BCGs, uniform grating, and 3-segment grating is also provided. Figure 3 illustrates the conversion bandwidths $\Delta\lambda$ versus the total waveguide length for different QPM structures. It can be seen that the bandwidths decrease as the length increases in all three gratings. Additionally, $\Delta\lambda$ of BCGs for waveguide lengths ranging from 1 cm to 5 cm are obviously greater than that of the others two gratings. For example, when the length increases from 3 cm to 4 cm, the $\Delta\lambda$ in BCGs structure is 155 nm which is 83 nm and 16 nm broader than that of uniform and 3-segment gratings, respectively. The reason for such excellent conversion bandwidth can be contributed to the fact that the BCGs structure has many reciprocal wave vectors. It is well known that, for QPM wavelength conversion, the phase matching condition is a crucial issue and generally must be satisfied to achieve good properties. However, in cascaded SHG + DFG-based devices using uniform grating, the SHG QPM condition is exactly satisfied, whereas the DFG process is mismatched especially when the difference between signal wavelength and pump wavelength becomes large. These will lead to limited conversion bandwidths. But, as just mentioned, the BCGs structure has large number of reciprocal wave vectors, which means that enough momenta can be provided to satisfy QPM conditions for both SHG and DFG simultaneously, though they are not exactly matched. As the result, the response can be broadened and flattened by optimizing the periods of BCGs.

The conversion efficiency and the flatness of response are other two important figures of merit for wavelength converters in the WDM systems. Therefore, both of them are quantitatively analyzed here for various waveguide lengths, as shown in Figs. 4. It can be seen from Fig. 4(a) that the maximum efficiency η_{max} of BCGs is less than that of the uniform and 3-segment gratings. However, the flatness F is better in comparison with the 3-segment grating and much closer to that of the uniform grating, and in some cases of 2.5-cm-, 4-cm- and 5-cm-long waveguide, the F of BCGs is even flatter than that of uniform grating, as shown in Fig. 4(b). Different conversion properties in uniform grating, 3-segment grating and BCGs result from different purposes of the poling periods designed for. Both the segmented grating and BCGs are designed to broaden conversion bandwidth, but the former in [10] is optimized to obtain high conversion efficiency simultaneously, whereas the latter in this paper is designed to achieve better response flatness at the same time. As a result, the BCGs shows better performances in bandwidth and flatness, while the η_{max} is smaller than the others.

#262298 Received 4 Apr 2016; revised 4 May 2016; accepted 6 May 2016; published 10 May 2016

Fortunately, we can easy enhance it by increasing the input pump power and/or using longer waveguide with some bandwidth penalty. For example, when the waveguide length is 3 cm and the pump power increases from 150 to 300 mW, the maximum efficiency will increases from −15.67 dB (2%$W^{-1}cm^{-2}$) to −10.27 dB (3.5%$W^{-1}cm^{-2}$). Furthermore, if we take advantage of 4-cm-long BCGs instead of the 3 cm one, though the bandwidth decreases from 180 nm to 155 nm, it is still large enough to cover most of the S-band, and the whole C- and L-bands, the enhancement of 4.6 dB in η_{max} can be achieved further; at the same time the response flatness of 0.54 dB in 4 cm waveguide is also better.

It is worth noting that the above results are simulated without considering waveguide loss. In fact, the propagation loss will degrade the conversion efficiency, but scarcely affect the bandwidth and the flatness [10,14]. Considering waveguide has loss and assuming them to be 0.35 dB/cm and 0.7 dB/cm for 1550-nm band and 775-nm band [26], respectively, if we still use 4-cm-long BCGs instead of the 3 cm one, the enhancement in maximum efficiency will decrease from 4.6 dB (without loss) to 4.0 dB. Moreover, the reduction in efficiency will becomes more relevant for increasing waveguide lengths, as shown in Fig. 4(a). This means, the improvement of the conversion efficiency, achieved by utilizing long loss-waveguide, will be weakened with the increase of waveguide length in comparison to the case without considering waveguide loss.

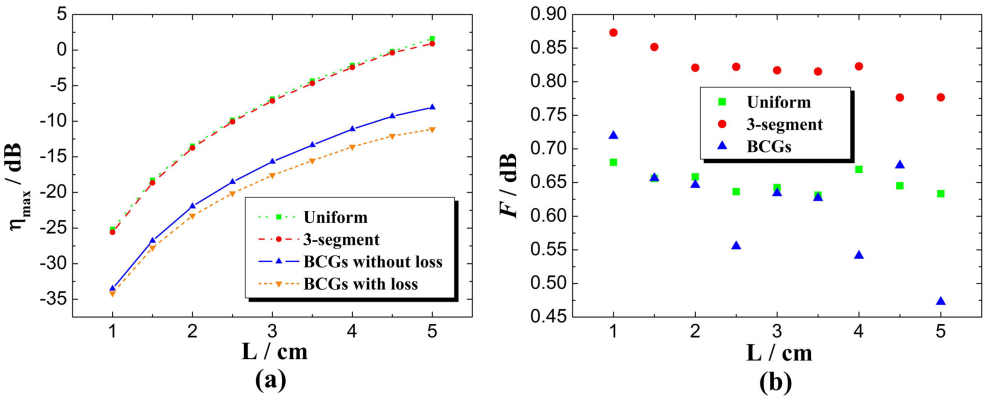

Fig. 4. Maximum conversion efficiencies (a) and response flatness (b) versus the total waveguide length in uniform grating, 3-segment grating and BCGs.

In the practical waveguide fabrication process, there exist manufacturing errors and some unpredictable factors which will both lead to a fluctuation of the length of fabricated gratings. The BCGs structure is, hence expected to be insensitive to the variation of length to make sure that similar conversion performances can be obtained. Thus, the manufacturing tolerance of the waveguide length is studied. Figure 5(a) shows the conversion efficiencies versus signal wavelength for BCGs with different waveguide total lengths. The periods used in Fig. 5(a) are all calculated by employing Eq. (1) and setting the chirp coefficients γ, τ and ξ to 0.00256, 11.2, and 7.2, which are utilized to achieve optimal conversion performances for a 3.5-cm-long waveguide above. As shown in Fig. 5(a), all parameters of interest: conversion bandwidth, maximum conversion efficiency and response flatness are waveguide length dependent. To clearly show the manufacturing tolerance of the BCGs structure, relative errors of the maximum conversion efficiency, bandwidth and flatness, corresponding to Fig. 5(a), are calculated and illustrated in Figs. 5(b)-5(d), respectively. In these figures, the horizontal axis denotes the deviation of waveguide lengths from 3.5 cm, the vertical axes are relative errors of η_{max}, $\Delta\lambda$ and F, respectively. It is easily seen from Figs. 5(b) and 5(c) that, if fabrication error is kept within 0.1 cm, the relative errors of η_{max} and $\Delta\lambda$ are less than 2.6% and 1.2%, respectively, which means almost the same maximum conversion efficiency and conversion bandwidth can be achieved compared to those of the ideal structure. Though the

#262298 Received 4 Apr 2016; revised 4 May 2016; accepted 6 May 2016; published 10 May 2016

relative errors of flatness for 3.4 cm and 3.6 cm BCGs are as high as −16.1% and 27.4%, respectively, as shown in Fig. 5(d), the flatness absolute values of them are still better than that of the 3-segment grating whose flatness is 0.82 dB for 3.5 cm waveguide at the same conditions. When the manufacturing error is larger than 0.1 cm, the response flatness will changes more rapidly. Based on the theory above we can conclude that the maximum manufacturing tolerance of waveguide length for BCGs structure should be smaller than 0.1 cm.

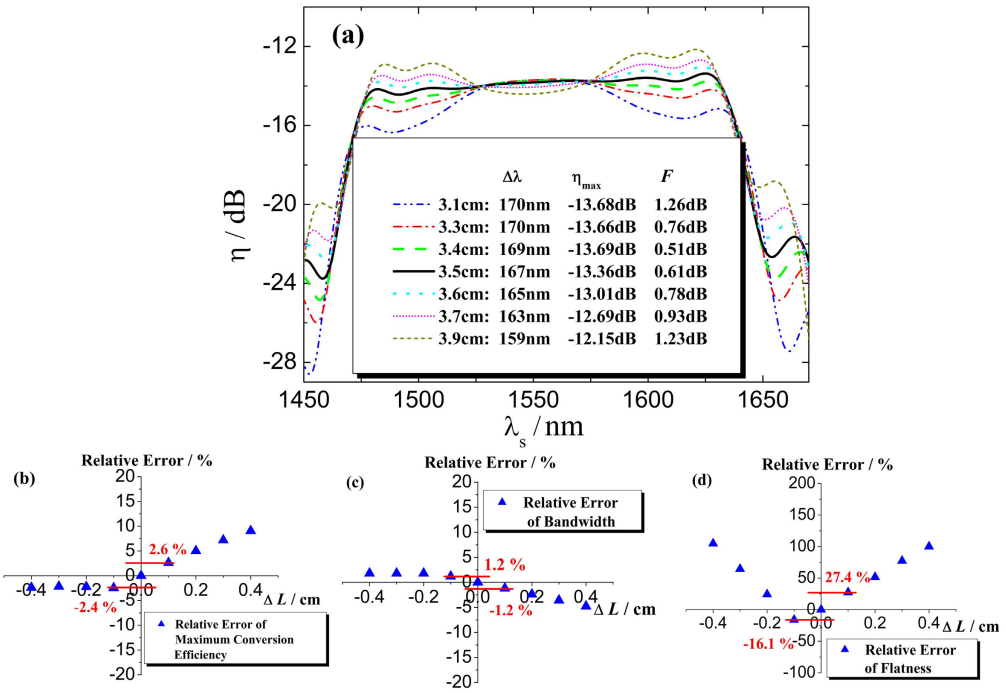

Fig. 5. (a) Conversion efficiencies versus signal wavelength for BCGs with the same poling period but different total waveguide lengths, and the corresponding relative errors of (b) η_{max}, (c) $\Delta\lambda$ and (d) F versus deviation of waveguide lengths from 3.5 cm.

4. Conclusion

A novel BCG structure has been proposed to broaden the bandwidth and flatten the response of wavelength converters based on cascaded SHG + DFG. Analyses show that the conversion bandwidth can be efficiently widened by employing this structure and optimizing its period, meanwhile the ripple on response can be made very small. A comparison among BCGs, uniform grating, and segmented grating is also performed, for various waveguide lengths, and demonstrates that BCG-based device has excellent bandwidth and better response flatness. As an illustrative example, for the 3-cm-long waveguide, the bandwidth and response flatness in BCG, uniform, and 3-segment gratings are 180 nm, 82 nm and 160 nm, and 0.62 dB, 0.64 dB and 0.82 dB, respectively. Although the maximum conversion efficiency of BCGs is smaller than that of the uniform and 3-segment gratings, it can be easily improved by enhancing the pump power and/or moderately increasing the waveguide length with some bandwidth penalty. Furthermore, when the manufacturing tolerance of the BCGs' length is smaller than 0.1 cm, almost the same conversion properties can be achieved. Therefore the proposed BCGs are suitable for the waveguide fabrication.

#262298 Received 4 Apr 2016; revised 4 May 2016; accepted 6 May 2016; published 10 May 2016

Acknowledgments

This work was supported by the National Natural Science Foundation of China (Grants Nos. 61302105 and 61302163), the Fundamental Research Funds for the Central Universities (Grants Nos. 2014MS99 and 13QN40), and the Science and Technology Research Foundation for Colleges and Universities in Hebei Province (Grants No. QN2016093).

#262298 Received 4 Apr 2016; revised 4 May 2016; accepted 6 May 2016; published 10 May 2016